

# A Potassium Tantalum(V) Tetrasilicate $\text{KTaSi}_2\text{O}_7$

Jong-Gyu Lee, Peter Höhn, and Martha Greenblatt<sup>1</sup>

Department of Chemistry, Rutgers, The State University of New Jersey, P.O. Box 939, Piscataway, New Jersey 08855-0939

Received February 17, 1995; in revised form January 23, 1996; accepted January 25, 1996

The crystal structure of a new potassium tantalum(V) cyclo-tetrasilicate,  $\text{KTaSi}_2\text{O}_7$  ( $\text{K}_2\text{Ta}_2\text{Si}_4\text{O}_{14}$ ), has been determined by single crystal X-ray diffraction.  $\text{KTaSi}_2\text{O}_7$  crystallizes in the tetragonal system, space group  $P4/mbm$  with  $a = 8.735(2)$  and  $c = 7.999(2)$  Å,  $V = 610.3(2)$  Å<sup>3</sup>,  $Z = 4$ ,  $d_x = 4.225$  g/cm<sup>3</sup>,  $\lambda$  (MoK $\alpha$ ) = 0.71073 Å,  $\mu = 190.7$  cm<sup>-1</sup>,  $F'(000) = 704$ ,  $T = 293$  K,  $R = 0.0421$ ,  $R_w = 0.0789$  for 451 unique reflections ( $R_{\text{int}} = 0.0227$ ) with  $F_0^2 > 0$ . The framework structure of  $\text{KTaSi}_2\text{O}_7$  is built up from chains of corner-sharing  $\text{TaO}_6$  octahedra running parallel to the fourfold axes and linked together by four-membered  $\text{Si}_4\text{O}_{12}$  single units. AC impedance measurements on  $\text{KTaSi}_2\text{O}_7$  indicate low ionic conductivities,  $5.6 \times 10^{-9}$  and  $3.0 \times 10^{-7}$   $\Omega \cdot \text{cm}^{-1}$  at 333 and 546°C, respectively. An activation energy of  $0.83 \pm 0.02$  eV is observed. © 1996 Academic

Press, Inc.

## INTRODUCTION

The chemistry and physics of reduced molybdenum, tungsten, and niobium oxides has been rich due to (i) the relative ease of preparation, (ii) low-dimensional structural properties with various tunnels, such as triangular, perovskitic, pentagonal, hexagonal, and octagonal, to accommodate a variety of ternary insertion elements, and (iii) anomalous electronic properties such as superconductivity, charge-density-wave and metal–insulator transition (1, 2, 3). There has been an interest in new reduced tantalum oxides analogous to the Nb, Mo, and W phases (4, 5). However, only a few reduced tantalum oxides are known, for example,  $\text{Ba}_3\text{Ta}_5\text{O}_{15}$  (5) and  $\text{Ba}_3\text{Ta}_6\text{Si}_4\text{O}_{23}$  (6).

The first tantalum rich disilicate compounds  $\text{Ba}_3\text{Ta}_6\text{Si}_4\text{O}_{23}$  and  $\text{Ba}_3\text{Ta}_6\text{Si}_4\text{O}_{26}$  were isolated by Shannon and Katz in 1970, when they attempted to prepare the reduced tantalum oxide  $\text{Ba}_{0.5}\text{TaO}_{3-x}$  (6, 7). The structure of  $\text{Ba}_3\text{Ta}_6\text{Si}_4\text{O}_{23}$  contains double layers of corner-shared  $\text{TaO}_5$  square pyramids and  $\text{Si}_2\text{O}_7$  disilicate units. The double layers of  $\text{TaO}_5$  are interleaved by barium ions. On the other hand,  $\text{Ba}_3\text{Ta}_6\text{Si}_4\text{O}_{26}$  has double layers of corner-shared  $\text{TaO}_6$  octahedra and  $\text{Si}_2\text{O}_7$  disilicate units (6, 8).

Both the oxidized and reduced phases contain pentagonal tunnels formed by three corner-shared  $\text{TaO}_6$  or  $\text{TaO}_5$  and two  $\text{Si}_2\text{O}_7$  polyhedra, which are commonly observed in tetragonal tungsten bronze structures, for example in  $\text{K}_x\text{WO}_3$  ( $x = 0.48\text{--}0.57$ ) (1, 2, 3). In  $\text{Ba}_3\text{Ta}_6\text{Si}_4\text{O}_{23}$ , tantalum is in the reduced oxidation state of 4+, possibly with  $d^1$  electronic configuration, but it is not a good conductor. The tantalum rich disilicate compounds,  $\text{K}_8\text{Ta}_{14}\text{Si}_4\text{O}_{47}$  and  $\text{K}_{6-2x}\text{Ba}_x\text{Ta}_6\text{Si}_4\text{O}_{26}$  ( $0 \leq x \leq 3$ ), were reported by Choynet *et al.* in 1977 (9).  $\text{K}_8\text{Ta}_{14}\text{Si}_4\text{O}_{47}$  is the first member ( $n = 1$ ) of the intergrowth series  $(\text{A}_x\text{Ta}_6\text{Si}_4\text{O}_{26})_n \cdot (\text{A}_y\text{Ta}_8\text{O}_{21})$ . The structure is related to that of  $\text{K}_6\text{Ta}_6\text{Si}_4\text{O}_{26}$  as evidenced by the transformation  $7\text{K}_6\text{Ta}_6\text{Si}_4\text{O}_{26} \rightarrow 3\text{K}_8\text{Ta}_{14}\text{Si}_4\text{O}_{47} + \text{K}_{18}\text{Si}_{16}\text{O}_{41}$  at 1350°C.

A reduced ternary tantalum oxide,  $\text{Ba}_3\text{Ta}_5\text{O}_{15}$ , was reported by Feger and Ziebarth in 1994 (5). It has the tetragonal tungsten bronze structure and shows semiconducting behavior with a resistivity several orders of magnitude higher than the isostructural Nb analog  $\text{Ba}_3\text{Nb}_5\text{O}_{15}$  (5).

Recently, Crosnier *et al.* have prepared  $\text{K}_2(\text{NbO})_2\text{Si}_4\text{O}_{12}$  with a three-dimensional skeleton structure as a candidate for fast alkali-ion conduction, such as Nasicon (10).  $\text{K}_2(\text{NbO})_2\text{Si}_4\text{O}_{12}$  crystallizes in the tetragonal system, space group  $P4bm$  with  $a = 8.7404(8)$  Å,  $c = 8.136(1)$  Å, and  $Z = 2$ . The structure is built up from chains of corner-shared  $\text{NbO}_6$  octahedra running parallel to the fourfold axes and linked together by four-membered  $\text{Si}_4\text{O}_{12}$  units. This structure is very similar to that of  $\text{K}_4(\text{ScOH})_2\text{Si}_4\text{O}_{12}$  (11).

In this paper, the refined single crystal structure of  $\text{KTaSi}_2\text{O}_7$  ( $\text{K}_2\text{Ta}_2\text{Si}_4\text{O}_{14}$ ), the crystals of which were grown during attempts to prepare precursors for tantalum phosphate bronze synthesis, is presented. The structure of  $\text{KTaSi}_2\text{O}_7$  is discussed in relation to the isostructural phase  $\text{K}_2(\text{NbO})_2\text{Si}_4\text{O}_{12}$  (10).

## EXPERIMENTAL

**Synthesis.** Single crystals of  $\text{KTaSi}_2\text{O}_7$  were grown from a mixture of  $2\text{K}_2\text{CO}_3$  (Johnson Matthey, ACS grade),  $3\text{Ta}_2\text{O}_5$  (Aldrich, 99%), and  $2(\text{NH}_4)_2\text{HPO}_4$  (ROC/RIC, 99+%). The reaction was performed in three steps. Ini-

<sup>1</sup> To whom correspondence should be addressed.

tially, the stoichiometric mixture was thoroughly mixed and then heated at 400°C for 4 h followed by calcination at 1050°C for 63 h in air. The calcined precursor was pressed into pellets and placed in doubly sealed quartz tubes. The samples were heated at 1030°C for 3 weeks, slowly cooled ( $\Delta T = -5^\circ\text{C}/\text{h}$ ) to 730°C and cooled to room temperature by turning off the power of the furnace. The crystals obtained are colorless rectangular needles. Their chemical analysis with an electron microprobe (Model JEOL-8600) indicated the presence of K, Ta, and Si. This analytical result indicated that the reaction product was a contaminated phase due to reaction with the fused silica tube. Polycrystalline  $\text{KTaSi}_2\text{O}_7$  was prepared by heating a powdered mixture of  $\text{K}_2\text{CO}_3$ ,  $\text{Ta}_2\text{O}_5$ , and  $\text{SiO}_2$  in a ratio of 1:1:4 at 1000°C/24 h, 1150°C/3 days, and 1300°C/3.5 days in air. The  $\text{KTaSi}_2\text{O}_7$  phase, unlike the Nb analog, did not form when heating was at  $\sim 1150^\circ\text{C}/3$  days.

**Powder XRD measurement.** Least-squares refinements of the powder X-ray diffraction (XRD) data of polycrystalline  $\text{KTaSi}_2\text{O}_7$  resulted in unit cell parameters  $a = 8.753(1)$  and  $c = 8.013(1)$  Å (space group =  $P4/mbm$ ). These unit cell parameters are slightly larger than those obtained on a CAD4 diffractometer,  $a = 8.735(2)$  and  $c = 7.999(2)$  Å for a single crystal of  $\text{KTaSi}_2\text{O}_7$ , and are similar to those of  $\text{K}_2(\text{NbO})_2\text{Si}_4\text{O}_{12}$ . Powder XRD patterns of the polycrystalline samples were also recorded both at low (77–298 K) and high (373–1273 K) temperatures on a SCINTAG PAD V diffractometer with low and high temperature devices.

**DTA measurement.** Possible phase transformations were investigated in polycrystalline samples in the temperature range 25–1500°C with a TA 2910 DTA (differential thermal analysis) cell in nitrogen flow.

**AC impedance measurement.** Ionic conductivities were measured in the temperature range 333–546°C in air by an ac impedance technique with a Solartron Model 1250 frequency analyzer and 1186 electrochemical interface that were equipped with a Hewlett Packard 9816 desktop computer for data collection and analysis. Electrode connections to the samples were made by coating the faces of the pellets with porous platinum.

**Single crystal X-ray data collection.** Diffraction data were collected at room temperature on an Enraf-Nonius CAD4 diffractometer. Crystallographic data for  $\text{KTaSi}_2\text{O}_7$  are summarized in Table 1. The single crystal X-ray study indicates that the new compound has tetragonal symmetry. The unit cell parameters and the orientation matrix were determined by a least-squares fit of 25 reflections; graphite-monochromatized  $\text{MoK}\alpha$  radiation was used for data collection in the range  $5 \leq 2\theta \leq 60^\circ$ . A  $\omega$ - $\theta$  scan mode was used. There was no detectable decay of intensity of the standard reflections during the data collection. Lorentz polarization and empirical absorption corrections, based

TABLE 1  
Crystallographic Data for  $\text{KTaSi}_2\text{O}_7$

Formula weight	388.23
Space group	$P4/mbm$ (No. 127)
Cell parameters	
$a$ (Å)	8.735(2)
$c$ (Å)	7.999(2)
$V$ (Å <sup>3</sup> )	610.3(2)
$Z$	4
$T$ (K) for data collection	293(2)
$\rho$ calculated (g · cm <sup>-3</sup> )	4.225
Radiation (Graphite monochromatized)	$\text{MoK}\alpha$ , $\lambda = 0.71073$ Å
Crystal shape, color	rectangular needle, colorless
Crystal size (mm)	$0.0875 \times 0.0875 \times 0.15$
Linear absorption coefficient (cm <sup>-1</sup> )	190.7
Scan type	$\omega$ - $\theta$
Scan speed (degree · min <sup>-1</sup> )	5.51 – 1.65°/min
Scan range (degrees)	$(1.40 + 0.30 \tan \theta)^\circ$
$2\theta$ range	$4^\circ$ – $60^\circ$
Data collected	$0 \leq h \leq 14$ , $0 \leq k \leq 9$ , $-12 \leq l \leq 0$
No. of reflections measured	632
No. of unique data	451
No. of unique data with $F_0^2 > 2\sigma(F_0^2)$	365
$F_{000}$	704
$R(F)^a$ , $R(F)$ for $F > 4\sigma(F)$	0.0421, 0.0308
$R_w(F^2)^b$	0.0789
$R_{\text{int}}$	0.0227
Goodness-of-fit <sup>c</sup>	1.098
Extinction coefficient	0.0053(5)
No. of variables	38

$$^a R(F) = \frac{\sum (|F_0| - |F_c|) / \sum |F_0|}{\sum |F_0|}$$

$$^b R_w(F^2) = \frac{[\sum \omega(|F_0| - |F_c|)^2 / \sum \omega |F_0|^2]^{1/2}}{\sum \omega |F_0|^2}; \omega = 1/(\sigma^2 |F_0|)$$

$$^c \text{G.O.F.} = \{\sigma(F_0^2 - F_c^2) / (N_{\text{obs}} - N_{\text{param}})\}^{1/2}$$

on three computer chosen azimuthal scans, were applied to the intensity data. The software packages SHELXS-86 and SHELXL-93 were used for the crystal structure solution and refinement, respectively.

## RESULTS AND DISCUSSION

**Structure determination.** An examination of the intensity data showed systematic absences characteristic of space groups  $P4/mbm$  (No. 127),  $P4bm$  (No. 100), and  $P4b2$  (No. 117):  $k = 2n + 1$  for  $0kl$  reflections. The structure determination was conducted in the centrosymmetric space group  $P4/mbm$ . Direct methods were used to obtain the initial positions of the heavy atoms Ta and K. The remaining atoms were found from successive Fourier maps. Refinement was carried out by the full-matrix least-squares method. At the completion of the refinement, the Ta atom—located on the fourfold axis, on a mirror plane—exhibited anomalously large anisotropic temperature fac-

TABLE 2  
Positional and Isotropic Parameters for  $\text{KTaSi}_2\text{O}_7$

Atom	Wyckoff notation	x	y	z	$U_{\text{eq}}$ ( $\text{\AA}^2$ )
Ta(1A)	4e	0	0	0.2262(4)	0.0060(4)
Ta(1B)	4e	0	0	0.2712(4)	0.0060(4)
Si	8k	0.3766(2)	0.1234(2)	0.6984(3)	0.0067(4)
K	4g	0.6774(3)	0.1774(3)	0	0.0207(6)
O(1)	2a	0	0	0	0.008(2)
O(2)	2b	0	0	0.5	0.014(3)
O(3)	4f	0.5	0	0.2263(8)	0.007(2)
O(4)	16l	0.2112(5)	0.0765(5)	0.2340(4)	0.013(1)
O(5)	4h	0.3818(8)	0.1183(8)	0.5	0.016(2)

Atom	$U_{11}$	$U_{22}$	$U_{33}$	$U_{12}$	$U_{13}$	$U_{23}$
Ta(1A)	0.0054(2)	0.0054(2)	0.007(1)	0	0	0
Ta(1B)	0.0054(2)	0.0054(2)	0.007(1)	0	0	0
Si	0.0056(6)	0.0056(6)	0.0090(8)	-0.0006(6)	0.0006(6)	-0.0002(8)
K	0.0221(9)	0.0221(9)	0.018(1)	0	0	-0.005(1)
O1	0.008(3)	0.008(3)	0.007(5)	0	0	0
O2	0.016(4)	0.016(4)	0.008(5)	0	0	0
O3	0.008(2)	0.008(2)	0.005(4)	0	0	0.003(3)
O4	0.005(2)	0.013(2)	0.019(2)	-0.001(2)	-0.001(2)	-0.004(2)
O5	0.022(3)	0.022(3)	0.005(3)	0	0	0.008(4)

tors along the fourfold axis. Subsequent refinement was therefore carried out with Ta located on a split position.

The crystal structure of  $\text{K}_2(\text{NbO})_2\text{Si}_4\text{O}_{12}$ , a compound with similar lattice constants and composition, has been reported; due to problems with the anisotropic temperature factors of some of the oxygen atoms in  $\text{K}_2(\text{NbO})_2\text{Si}_4\text{O}_{14}$  the structure was refined in the acentric space group  $P4bm$  (10). Attempts to refine  $\text{K}_2(\text{TaO})_2\text{Si}_4\text{O}_{12}$  (i.e.,  $\text{KTaSi}_2\text{O}_7$ ) in space groups  $P4b2$  and, with lower Laue symmetry,  $P4/m$ ,  $P4$ , and  $P\bar{4}$  were not successful, even if the crystal was regarded as a twin and a twinning matrix was applied. The resulting  $R$  values were always worse than in the centrosymmetric refinement, and in every case, some of the oxygen atoms could not be refined anisotropically. When the Ta atom was retained in a split position, similar results were obtained in both centrosymmetric ( $P4/mbm$ ) and noncentrosymmetric ( $P4bm$ ) space groups; all refinements in the acentric space group resulted in  $R$  values equal to those in the centrosymmetric refinement. In addition, the anisotropic temperature factors did not improve. Therefore, since the refinement in the acentric space group did not improve the structure model, refinement in  $P4/mbm$  was chosen.

The positional parameters of the nine unique atoms and their anisotropic temperature factors were refined to  $R_w = 0.0789$ ,  $R(4\sigma) = 0.0308$ , and  $R$  (all reflections) = 0.0421 (see Table 2); all temperature factors are observed within expected values. The final difference Fourier map is featureless with maxima and minima in the range  $+2.03/-1.29$

$e/\text{\AA}^3$ . The highest value is observed near Ta. Structure factor tables and further information may be obtained upon request.<sup>2</sup>

*Description of the structure.* The crystal structure, depicted as a polyhedral representation in Fig. 1, may be described as consisting of chains of corner-sharing  $\text{TaO}_6$  octahedra running parallel to the fourfold axis. The chains are connected by four-membered  $\text{Si}_4\text{O}_{12}$  units so that each octahedron shares four corners with four  $\text{SiO}_4$  tetrahedra belonging to four different  $\text{Si}_4\text{O}_{12}$  units (Fig. 2). All  $\text{Si}_4\text{O}_{12}$  units are located at the same height ( $z$ ) resulting in Si-O double layers (Fig. 1). The Si atoms in the  $\text{Si}_4\text{O}_{12}$  units are connected via O3 and O5, whereas each O4, located at the eight outward-pointing vertices of the  $\text{Si}_4\text{O}_{12}$  unit, joins with the  $\text{TaO}_6$  octahedron so that each  $\text{Si}_4\text{O}_{12}$  unit links four different chains to yield the three-dimensional network crystal structure. This arrangement results in channels that extend through the structure in the  $[001]$  direction, where

<sup>2</sup> See NAPS document No. 05292 for 07 pages of supplementary materials. Order from ASIS/NAPS, Microfiche Publications, P.O. Box 3513, Grand Central Station, New York, NY 10163. Remit in advance \$4.00 for microfiche copy or for photocopy, \$7.75 up to 20 pages plus \$0.30 for each additional page. All orders must be prepaid. Institutions and Organizations may order by purchase order. However, there is a billing and handling charge for this service of \$15. Foreign orders add \$4.50 for postage and handling, for the first 20 pages, and \$1.00 for additional 10 pages of material, \$1.50 for postage of any microfiche orders.

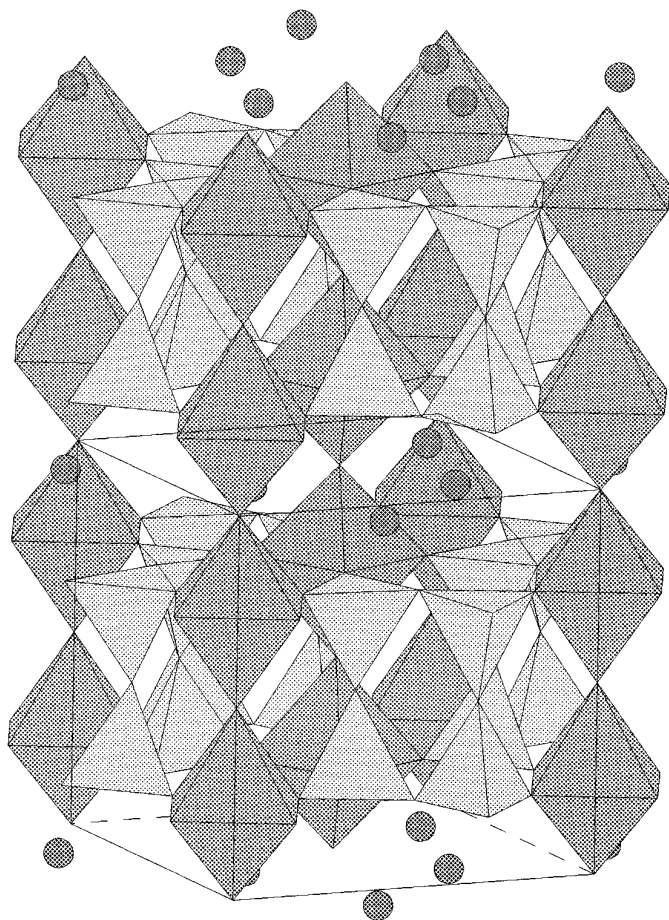
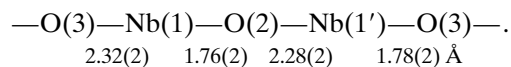


FIG. 1. Crystal structure of  $\text{KTaSi}_2\text{O}_7$ . The  $\text{Si}_4\text{O}_{12}$  units are located at the same height along the  $c$  axis.  $\text{K}^+$  ions are positioned between the  $\text{Si}_4\text{O}_{12}$  units in the pentagonal tunnels.

the potassium atoms are located exclusively. The  $\text{K}^+$  ions are positioned between  $\text{Si}_4\text{O}_{12}$  units in the pentagonal tunnels, leaving the possible cation positions within the  $\text{Si}_4\text{O}_{12}$  units unoccupied and therefore indicating only half occupancy. It is noteworthy that in  $\text{K}_4(\text{ScOH})_2\text{Si}_4\text{O}_{12}$  (simplified as  $\text{K}_2\text{ScSi}_2\text{O}_6\text{OH}$ ), which is isostructural with  $\text{KTaSi}_2\text{O}_7$ , the pentagonal tunnels are fully occupied by  $\text{K}^+$  ions. Similarly, while the cation positions in  $\text{K}_6\text{Ta}_6\text{Si}_4\text{O}_{26}$  are fully occupied, in the isostructural  $\text{Ba}_3\text{-Ta}_6\text{Si}_4\text{O}_{26}$  compound, they are half filled.

Bond distances, bond angles, and their standard deviations are listed in Table 3. The  $\text{TaO}_6$  octahedra are nearly regular with O–O distances ranging from 3.926 to 4.000 Å. The Ta atoms within these octahedra are displaced from the center by about 0.16–0.19 Å, resulting in different Ta–O bond lengths (Fig. 3). For each Ta, five short (Ta(1A): 1.810(3),  $4 \times 1.963(4)$  Å; Ta(1B): 1.830(4),  $4 \times 1.984(4)$  Å) and one long Ta–O distance (Ta(1A): 2.190(3); Ta(1B): 2.169(3) Å) are observed.

There appear to be long and short Ta–O distances (Ta(1A)–O: 1.810(3)/2.190(3) Å; Ta(1B)–O: 1.830(3)/2.169(3) Å) along the  $c$  axis. Because the occupancy factor of each Ta position is 0.5, there is exactly one Ta atom located in each  $\text{TaO}_6$  octahedron. Since X-ray diffraction methods average over the whole crystal, the crystal has to be regarded as containing domains of octahedral chains with alternating long and short Ta–O distances facing up and down (i.e., each Ta along the chain is moved either up or down from its ideal position), as well as short–short and long–long Ta–O distances in a statistically disordered fashion (i.e., alternating Ta's are moved up and down respectively from their ideal position (0, 0, 1/4)). Space group  $P4bm$  would allow only alternating short and long Ta–O distances along the  $c$  direction, but the structure refinement is not able to predict unambiguously which case exists. In contrast to the disorder of Ta atoms observed in  $\text{KTaSi}_2\text{O}_7$ , in  $\text{K}_2(\text{NbO})_2\text{Si}_4\text{O}_{12}$ , which crystallizes in space group  $P4bm$ , only a sequence of alternating short and long Nb–O distances along the fourfold axis is observed:



However, the  $\text{NbO}_6$  octahedra are more distorted in  $\text{K}_2(\text{NbO})_2\text{Si}_4\text{O}_{12}$  than the  $\text{TaO}_6$  octahedra in  $\text{KTaSi}_2\text{O}_7$ . The different behavior of Ta versus Nb is probably due to

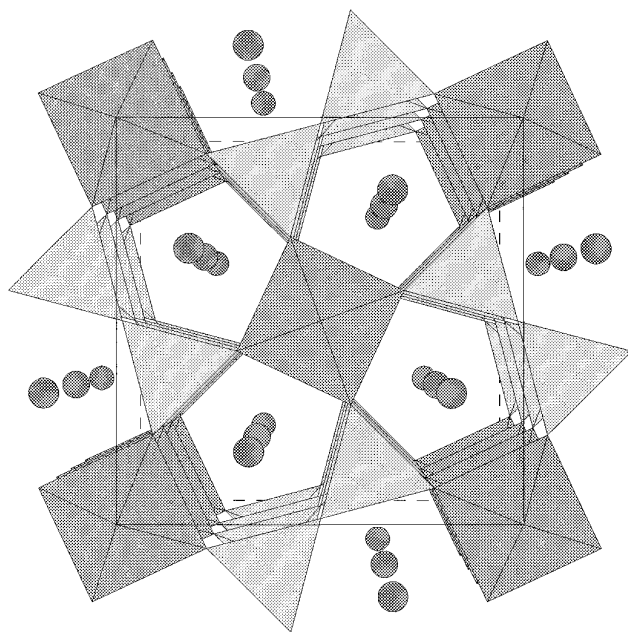


FIG. 2. Perspective [001] view of  $\text{KTaSi}_2\text{O}_7$ . Two  $\text{TaO}_6$  octahedra and three  $\text{SiO}_4$  tetrahedra form a pentagonal tunnel along the  $c$  axis, where  $\text{K}^+$  ions are positioned.

TABLE 3  
Bond Distances and Angles (Degrees) for the TaO<sub>6</sub>  
Octahedra and SiO<sub>4</sub> Tetrahedra in KTaSi<sub>2</sub>O<sub>7</sub>

Ta(1A, 1B)O <sub>6</sub> octahedra			
Ta(1A)–O(1)	1.810(3)	Ta(1B)–O(1)	2.169(3)
Ta(1A)–O(2)	2.190(3)	Ta(1B)–O(2)	1.830(3)
Ta(1A)–O(4)	1.963(4) (4 ×)	Ta(1B)–O(4)	1.984(4) (4 ×)
O(1)–Ta(1A)–O(4)	91.8(1) (4 ×)		
O(4)–Ta(1A)–O(4)	89.94(1) (4 ×)		
O(1)–Ta(1A)–O(2)	180.0		
O(4)–Ta(1A)–O(2)	88.2(1) (4 ×)		
O(4)–Ta(1A)–O(4)	176.4(3) (2 ×)		
O(2)–Ta(1B)–O(4)	98.6(1) (4 ×)		
O(4)–Ta(1B)–O(4)	88.71(4) (4 ×)		
O(2)–Ta(1B)–O(1)	180.0		
O(4)–Ta(1B)–O(1)	81.4(1) (4 ×)		
O(4)–Ta(1B)–O(4)	162.7(3) (2 ×)		
Ta(1A)–O(1)–Ta(1A)	180.0		
Ta(1A)–O(1)–Ta(1B)	180.0		
Ta(1B)–O(1)–Ta(1B)	180.0		
Ta(1A)–O(2)–Ta(1A)	180.0		
Ta(1B)–O(2)–Ta(1A)	180.0		
Ta(1B)–O(2)–Ta(1B)	180.0		
SiO <sub>4</sub> tetrahedra			
Si–O(3)	1.639(3)	Si–O(5)	1.588(2)
Si–O(4)	1.597(4) (2 ×)		
O(3)–Si–O(5)	109.3(4)	Si–O(3)–Si	136.8(4)
O(4)–Si–O(3)	107.6(2) (2 ×)	Si–O(5)–Si	175.5(7)
O(4)–Si–O(4)	110.5(3)		
O(4)–Si–O(5)	110.9(2) (2 ×)		
KO <sub>12</sub> polyhedra			
K–O(1)	3.216(1) (2 ×)		
K–O(3)	2.842(5) (2 ×)		
K–O(4)	2.865(5) (4 ×)		
K–O(4)	3.061(4) (4 ×)		

the slightly more ionic character of the Ta–O bond, which would result in a tendency to get a more symmetrical octahedral coordination. As noted above, no transition to either a more ordered or more disordered form at low or high temperatures is observed.

The SiO<sub>4</sub> tetrahedron is quite regular with Si–O bond lengths in the range from 1.588(2) to 1.639(3) Å, the average distance being 1.605 Å, and the O–Si–O angles range from 107.6(2)° to 110.9(2)°. The Si and the bridging O(3,5) atoms are located on a mirror plane with Si–O–Si angles 136.8(4)° and 175.5(7)°, respectively. The Si<sub>4</sub>O<sub>12</sub> unit can be regarded as an association of two Si<sub>2</sub>O<sub>7</sub> units in eclipsed configuration (Fig. 3). These framework units are also observed in K<sub>2</sub>(NbO)<sub>2</sub>Si<sub>4</sub>O<sub>12</sub> and K<sub>4</sub>(ScOH)<sub>2</sub>Si<sub>4</sub>O<sub>12</sub> (10, 11); however, the average Si–O bond lengths are slightly shorter (1.605 Å) in the Ta than those in the Nb (1.610 Å) analog.

**Thermal analysis.** Polycrystalline samples of KTaSi<sub>2</sub>O<sub>7</sub> show no evidence of structural change in powder XRD

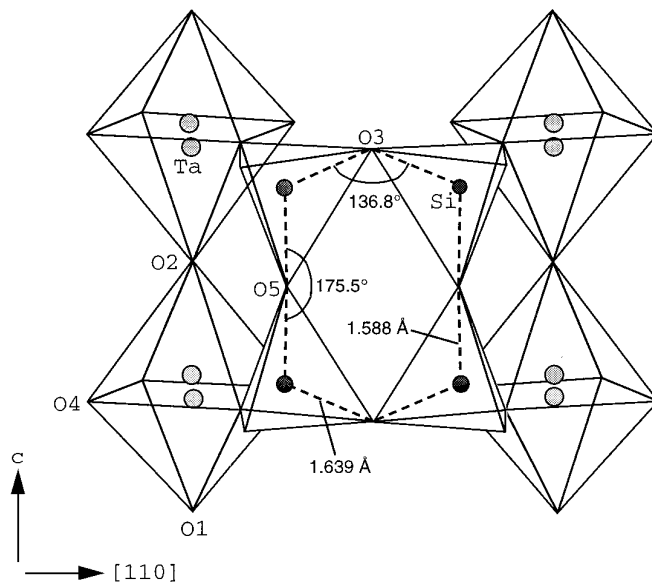


FIG. 3. Crystal structure of KTaSi<sub>2</sub>O<sub>7</sub> viewed along the [110] direction. Ta atoms within TaO<sub>6</sub> octahedra are displaced from the center by ~0.16–0.19 Å. The Si and the bridging O(3,5) atoms are located on a mirror plane with Si–O–Si angles of 136.8(4)° and 175.5(7)°, respectively.

patterns recorded at low (77–298 K) and high (373–1273 K) temperatures. Further, no evidence of structural change was observed by high-temperature DTA from 25 to 1500°C. KTaSi<sub>2</sub>O<sub>7</sub> melts incongruently at 1371°C.

**Ionic conductivity.** A sintered polycrystalline sample KTaSi<sub>2</sub>O<sub>7</sub> showed very low ionic conductivities ( $\sigma$ ) of  $5.6 \times 10^{-9}$  and  $3.0 \times 10^{-7} \Omega^{-1} \cdot \text{cm}^{-1}$  at 333 and 546°C, respectively. The activation energy ( $E_a$ ) is  $0.83 \pm 0.02$  eV. The low ionic conductivity observed is attributed to the one-dimensional ionic motion along the *c* axis (Fig. 2); in a polycrystalline sample an average of the ionic conductivity is observed.

## ACKNOWLEDGMENTS

The authors thank Dr. Tom Emge for the data collection and Mr. J. Yan for the ionic conductivity measurement. We thank Professor W. H. McCarrroll for critically reading the manuscript. This work was supported by NSF Solid State Chemistry Grants DMR-91-19301 and DMR-93-14605.

## REFERENCES

1. M. Greenblatt, *Chem. Rev.* **88**, 31 (1988); M. Greenblatt, *Int. J. Mod. Phys. B* **7**(23–24), 3937 (1993); M. M. Borel, M. Goreaud, A. Grandin, Ph. Labbe, A. Leclaire, and B. Raveau, *Eur. J. Solid State Inorg. Chem.* **28**, 93 (1991).
2. A. Manthiram and J. Gopalakrishnan, *Rev. Inorg. Chem.* **6**, 1 (1984).

3. J. Köhler, G. Svenssen, and A. Simon, *Angew. Chem. Int. Ed. Engl.* **31**, 1437 (1992).
4. F. Galasso, L. Katz, and R. Ward, *J. Am. Chem. Soc.* **81**, 5898 (1959).
5. C. R. Feger and R. P. Ziebarth, *Chem. Mater.* **7**, 373 (1995).
6. J. Shannon and L. Katz, *J. Solid State Chem.* **1**, 399 (1970).
7. J. Choisnet, N. Nguyen, D. Groult, and B. Raveau, *Mater. Res. Bull.* **11**, 887 (1976).
8. D. P. Birkett, P. J. Wiseman, and J. B. Goodenough, *J. Solid State Chem.* **37**, 6 (1981).
9. J. Choisnet, N. Nguyen, and B. Raveau, *Mater. Res. Bull.* **12**, 91 (1977).
10. M. P. Crosnier, D. Guyomard, A. Verbaere, Y. Piffard, and M. Tournoux, *J. Solid State Chem.* **98**, 128 (1992); *Ferroelectrics* **124**, 51 (1991).
11. Yu. A. Pyatenko, T. A. Zhdanova, and A. A. Voronkov, *Sov. Phys. Dokl. Engl. Transl.* **24**, 794 (1979).